Optimization of a Prototype Atomic Clock Based on Coherent Population Trapping

Nathan Belcher *REU program, College of William and Mary*
I. Novikova *College of William and Mary, Physics Department*

August 1, 2008

Abstract

The goal of this project is to optimize parameters of a prototype atomic clock to achieve the best Allan variance. We have established a prototype atomic clock using coherent population trapping (CPT) by creating a laser system to lock the laser's frequency to an atomic resonance in rubidium and utilized radiofrequency (rf) modulation to create a sideband and carrier comb. With the system assembled, we have achieved our best Allan variance of 4×10^{-10} for a 15 torr Neon buffer gas cell, but have changed to a 5 torr Neon buffer gas cell to decrease the Allan variance.

1 Introduction

In the last decade, advances have been made in creating miniature (sub-cubic centimeter) atomic clocks, based on laser probing of an atomic vapor. The laser employed in these clocks is a vertical-cavity surface-emitting laser (VCSEL), which has useful characteristics for this application: low power consumption, ease of current modulation with radiofrequency (rf) signals, and use in minature atomic clocks.

The atomic clocks contain three parts: a hyperfine transition (in the microwave region) between two long-lived spin states of an alkali metal (that has a hydrogen-like spectrum), a frequency modulator with counter, and a laser. The element of use in this atomic clock is rubidium, which is an alkali metal. The frequency modulator provides phase modulation, creating two electro-magnetic fields at different frequencies out of one physical laser. A counter matches the frequency driven by the modulator to give a reference for time, and the laser drives the entire process. To keep the laser at a set frequency corresponding to the atomic transition, another part called a dichroic atomic vapor laser locking (DAVLL) system is needed. The DAVLL uses an error signal determined by the difference of signal in two photodetectors to keep the laser's frequency on a rubidium resonance. In addition, electronics of the frequency modulator keep the modulation frequency at the "clock" frequency, allowing an atomic clock to be created for an extended period of time.

The overall goal of this project is to optimize the performance a prototype atomic clock. This paper describes the following: theories underlying the atomic clock in section 2; the experimental setups in section 3; first coherent population trapping (CPT) lineshape results in section 4; first clock results in section 5; second CPT lineshape results in section 6; and second clock results in section 7.

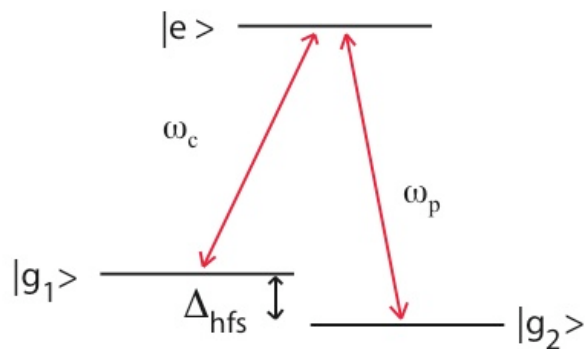# 2   Theory

2.1   Coherent Population Trapping

Figure 1: A Λ system. Levels g_1 and g_2 are states in $5S_{1/2}$ separated by the hyperfine splitting (6.834 GHz), and level e is 794.7 nm away from the $5S_{1/2}$ state.

The driving mechanism of the clock is a phenomenon known as CPT. It is created from a three-level system (specifically a Λ system, see figure 1) by matching the hyperfine frequency difference of the two rubidium ground states (Δ_{hfs}) with frequency difference from two electromagnetic fields. The three-level system consists of two ground states $|g_1\rangle$ and $|g_2\rangle$ separated by an energy $\hbar\Delta_{hfs}$ and a single excited state $|e\rangle$. When the frequency differece of ω_c and ω_p matches the frequency of the hyperfine splitting between the two ground states, a "dark" state is formed. It is known as the dark state because atoms in it will not absorb either electromagnetic field, giving almost 100 percent transmission. The equation is:

$$|dark\rangle = \frac{\Omega_1 |g_2\rangle - \Omega_2 |g_1\rangle}{\sqrt{|\Omega_1|^2 + |\Omega_2|^2}} \qquad (1)$$

where Ω_1 and Ω_2 are the Rabi frequencies of the two transitions. For a much further mathematical treatment of the dark state, see [1].

2.2 Phase Modulation

Because CPT is very sensitive to frequency difference between two laser fields in the Λ system, a few problems exist. The first problem is the laser will move around a set frequency in a random way ("jump"), regardless of the quality of the laser. If two physically separate lasers are used at two different frequencies, they will both jump randomly and not have any correlation. To correct this problem, two lasers can be created out of one physical laser by modulating its phase. The relative frequency of the two fields can be set by an external generator, and this creates a carrier with sideband comb. Even though there will still be jumps around the set frequency, both laser fields will jump in the same way.

The mathematics behind phase modulation is useful. A generic electromagnetic wave described by the following equation

$$E = E_0 e^{ikx - i\omega t + i\varphi(t)} \tag{2}$$

where E_0 is the amplitude of the wave, ω is the phase, and k is a vector that points in the direction the wave is traveling. Phase $\varphi(t)$ is the modulated in the form

$$\varphi(t) = \varepsilon sin(\omega_m t) \tag{3}$$

where ε is the amplitude of modulation and ω_m is the modulation frequency. Taking a Bessel function decomposition of φ into E gives the final result of:

$$E = \sum_{n=0}^{\infty} E_0 J_n(\varepsilon) e^{ikx - i(\omega - n\omega_m)t} \tag{4}$$

This equation is the basis for the carrier and sideband comb, because the frequency difference between the carrier and each nth sideband is determined by $\omega - n\omega_m$.

An advantage of using the VCSELs is that their output can be phase-modulated by direct current modulation up to relatively high (10 GHz) frequencies. In addition, phase modulation allows matching of the hyperfine splitting in the rubidium vapor at 6.834 GHz.

3 Experimental Setup

To create CPT and the clock, much work has been performed. For an in-depth analysis of each part in the experimental setup, please refer to [1].

3.1 CPT Experimental Setup

The first part of the clock is creating a CPT peak that will serve as our reference signal. To do this, we follow the schematic in figure 2. The laser is first phase modulated at the same frequency as the hyperfine splitting of the ground states (6.834 GHz), and then sent through the rubidium cell and into a photodetector. The laser is split before the rubidium cell and also sent to the DAVLL system, which locks the laser
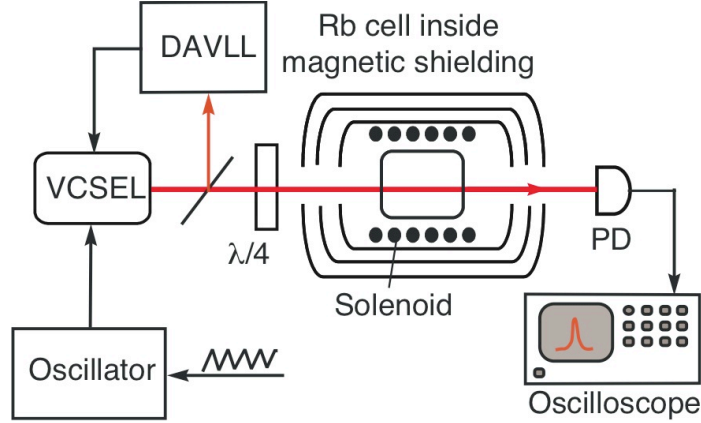
Figure 2: Setup schematic for the CPT experiment.

to the optical frequency between the ground and excited states. In addition, before the rubidium cell is a half waveplate and polarizing cube, to give smooth tuning of the laser power. We read the signal from the photodetector on an oscilloscope, and record the signal from the oscilloscope with a LabView program.
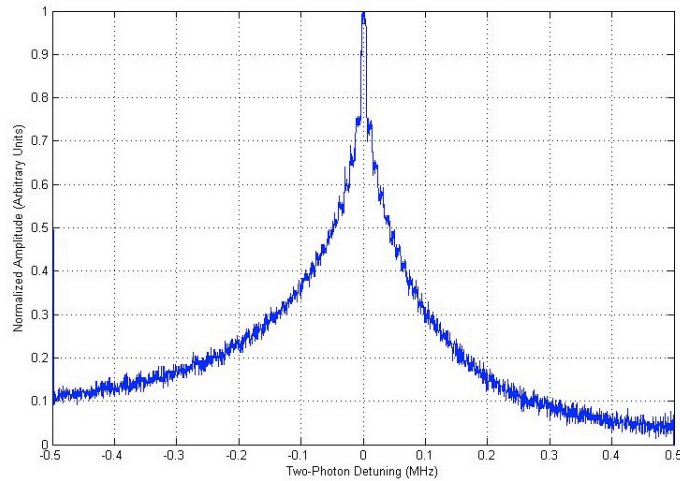

Figure 3: Single CPT peak with 1 MHz slow modulation sweep of the phase modulation.

Figure 3 is an example of a signal that is seen on the oscilloscope when we have achieved CPT. When the frequency of the phase modulation matches the hyperfine splitting frequency and the optical frequency is locked by the DAVLL system, the atoms are in a dark state and we see transmission of the laser through the rubidium cell. The laser is swept with an added modulation (1 MHz in figure 3) through the central frequency, so we can see detuning from dark state. After recording each peak, we analyze them with a program called IgorPro. We use this program to fit the peaks with a function (normally generalized Lorentzian), and create a set of raw data containing background, two-photon detuning, amplitude, and width of each peak.

4

The raw data is then collected and presented in a format that is more readable, and also graphed versus laser power.
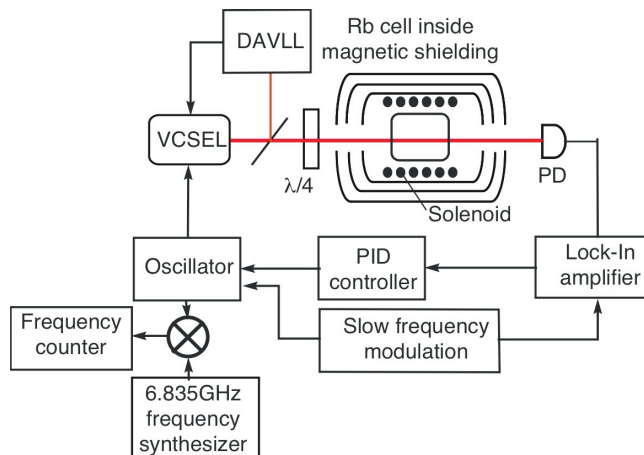
3.2   Clock Experimental Setup

Figure 4: The clock experimental setup.

To create the clock, we take the CPT setup and add a few parts (refer to figure 4). Again, the laser is phase modulated at the same frequency as the hyperfine splitting of the ground states (6.834 GHz), but the modulation is set with a PID controller. Slow frequency modulation is added to the modulation from the PID controller and also sent to a lock-in amplifier, which acts a narrow bandpass filter to provide a feedback signal for the PID controller. The laser is again split before the rubidium cell and also sent to the DAVLL system, which locks the laser to the optical frequency between the ground and excited states. The signal from the oscillator (a combination of slow frequency modulation and modulation at the hyperfine splitting frequency) is sent to a mixer, which also takes in a signal from a stable reference frequency. The two signals are beaten together, analyzed by a frequency counter, and recorded with a LabView program. The frequency of the beats determines the accuracy of the clock, which is given in a form known as the Allan variance.

4   First CPT Lineshape Results

With the experimental process described in the CPT experimental section, CPT peaks were taken with LabView. The goal was to move through our parameter space of temperature and rf power, and find the optimal CPT resonance given changing laser power. Four different temperatures were used (40, 45, 50, and 58 degrees Celsius), and rf powers giving sideband percentages ((sideband/carrier)*100) of 30, 60, and 90 were also used for each temperature. Each peak at a specific temperature, rf power, and laser power was analyzed with IgorPro, and background, amplitude,

two-photon detuning, and width were extracted. Three other parameters were calculated: contrast (amplitude/background), amplitude/width, and contrast/width. The optimal CPT resonance has maximal amplitude, contrast, amplitude/width, and contrast/width, minimal width, and no two-photon detuning. Two-photon detuning is associated with rf power, and amplitude, background, and width are associated with temperature of the rubidium cell.

After analyzing the data at the four temperatures, we decided the best temperature to use would be 45 degrees Celsius. The main reason 45 degrees Celsius was chosen is seen in the two-photon detuning graph (figure 5), because at this temperature 90 percent sidebands give a flat line. The flat line means the two-photon detuning does not change for changing laser power (known technically as lightshift cancellation), which is a necessary condition for the miniature atomic clocks. The miniature atomic clocks cannot guarantee a constant laser power, so to keep the clock system locked we need the place where varying laser power is not an issue. We then took data again with four different input rf powers at sideband percentages of 60, 80, 90, and 100. Figures 5 through 10 are the data at 45 degrees Celsius with different rf powers.

After consulting these figures, we decided to lock our clock with 90 percent sidebands. The 90 percent sidebands data had the lightshift cancellation, and is also comparable to the others in width, amplitude, contrast, amplitude/width, and contrast/width.
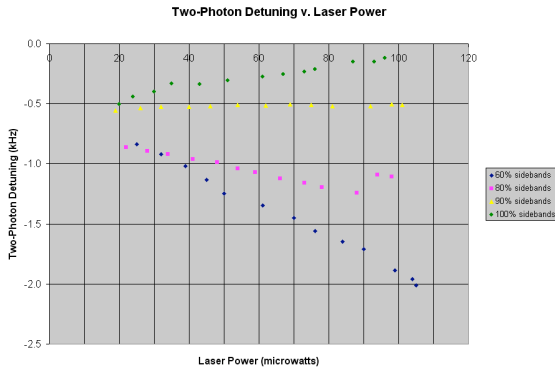

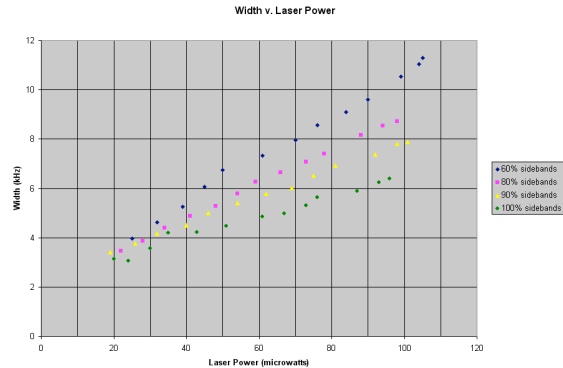Figure 5: Two-photon detuning versus laser power.
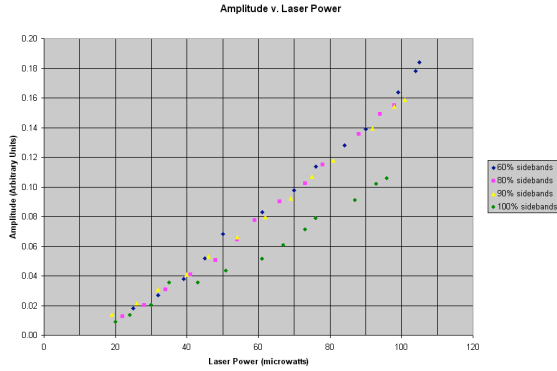

Figure 6: Width versus laser power.

6

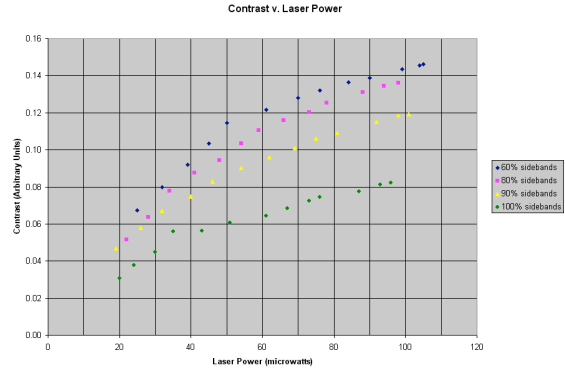Figure 7: Amplitude versus laser power.

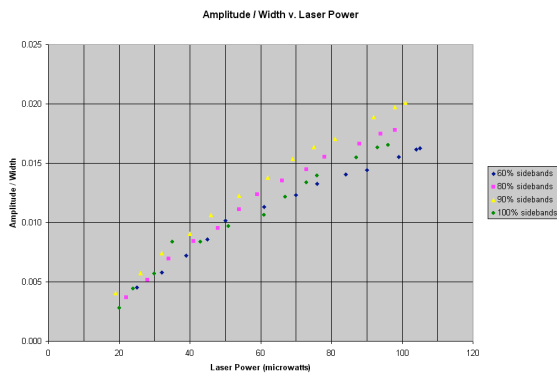Figure 8: Contrast versus laser power.

Figure 9: Amplitude/width versus laser power.

Figure 10: Contrast/width versus laser power.

5   First Clock Results

Before creating the clock, another set of data needed to be taken. In the clock setup, a lock-in amplifier produces a steep anti-symmetric curve (figure 11), and we wanted to find the modulation depth and modulation frequency that would produce the largest slope. We changed the modulation depth and modulation frequency with the synthesizer, and found values for each combination for three different currents through the solenoid surrounding the rubidium cell: 6 mA, 16 mA, and 26 mA. These values were then compiled into contour plots with the x-axis modulation frequency, y-axis modulation depth, and z-axis height of slope (figures 12 through 14), and used to find the best locking point for each current. More height of slope is better for locking, so we found each current had the best locking point around 3 kHz modulation frequency and 4 kHz modulation depth. The 26 mA current error slope had another locking point around 3 kHz modulation frequency and 2 kHz modulation depth, which could also be used in the clock.

After performing the work on the error slope, we locked the clock with the setup given in the experimental setup section. The main way to characterized the performance of the clock is with an equation known as the Allan variance, which is given
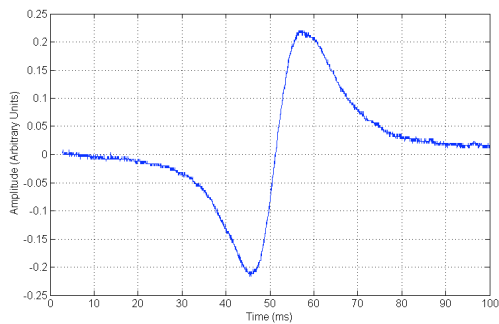
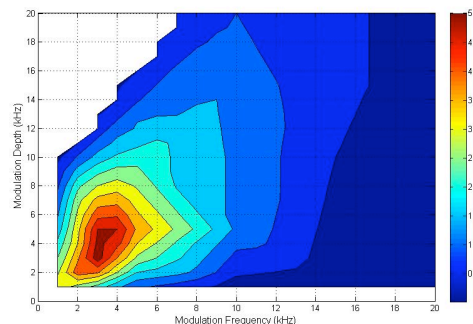Figure 11: Error slope produced by lock-in amplifier.

Figure 12: Contour plot of lock-in error slope data for 6 mA of current.
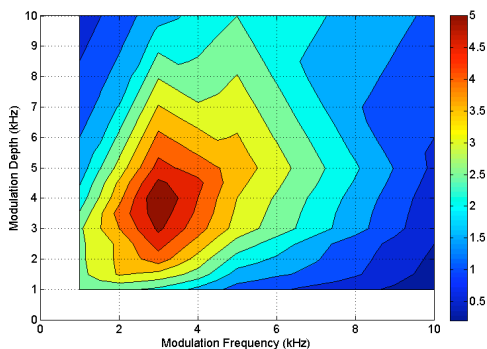

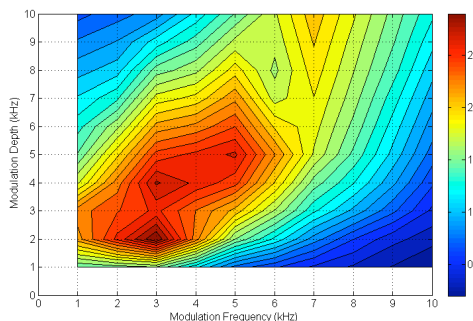Figure 13: Contour plot of lock-in error slope data for 16 mA of current.

Figure 14: Contour plot of lock-in error slope data for 26 mA of current.

by the equation:

$$\sigma_\nu^2(\tau) = \frac{1}{2} \left\langle \nu^2 \right\rangle \tag{5}$$

It says that for each time interval τ, the expectation value of ν is calculated. The variable ν is the difference in the measures of each succesive frequency; *i.e.* if i denotes the ith measurement of ν, then $\nu = (\nu_i + 1) - \nu_i$. Each adjacent difference of ν is then squared and averaged over a given time period, and finally divided by two. The divide by two causes this variance to be equal to the classical variance if the data is taken from a random and uncorrelated set (also known as white noise). In addition, Allan variance is a unitless quantity.

We had created a clock during the spring semester, and managed to achieve a short-term stability of 8×10^{-12} and total locking time of 41 hours with a 6 Hz drift. This was with the rubidium transition of F=1 to F'=2, but we really want to use the F=2 to F'=1 transition (known hereafter as the F=2 transition). The F=2 transition is useful because it is magnetically invariant, meaning the amplitude doesn't change for changing magnetic fields. This is important in the miniature atomic clocks, because they are not shielded very well from inhomogenous magnetic fields. With the F=2 transition and the CPT parameters defined in the previous section (rubidium

cell temperature, rf power, etc.), we achieved our best Allan variance of 4×10^{-10}. This is significantly less than we hoped for, and caused us to change rubidium cells from one with 15 torr of Neon buffer gas pressure to a 5 torr Neon buffer gas pressure cell. Figures 15 and 16 are the best Allan variance and its corresponding data figure.
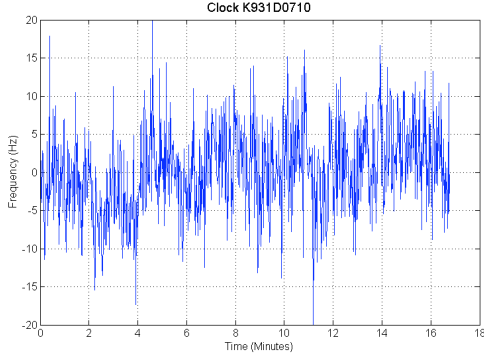

Figure 15: Data figure corresponding to the best Allan variance for the F=2 transition.
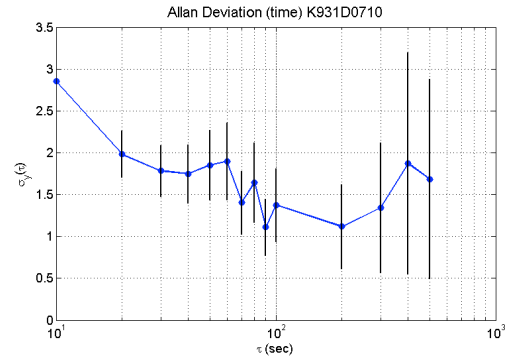

Figure 16: Best Allan variance achieved for F=2 transition. The lowest dot corresponds to 4×10^{-10} Allan variance.

6   Second CPT Lineshape Results

After changing the rubidium cells from 15 torr Neon to 5 torr Neon, the CPT lineshape data had to be retaken. With the same description of data collection and analysis from the First CPT Lineshape section, we gathered the data. We first found the rf power that gave lightshift cancellation, and with the 5 torr cell cancellation happened with 75 percent sidebands. We then compiled the data taken over five different temperatures (35, 40, 45, 48, 53, and 56 degrees Celsius), and figures 17 through 22 show the data.
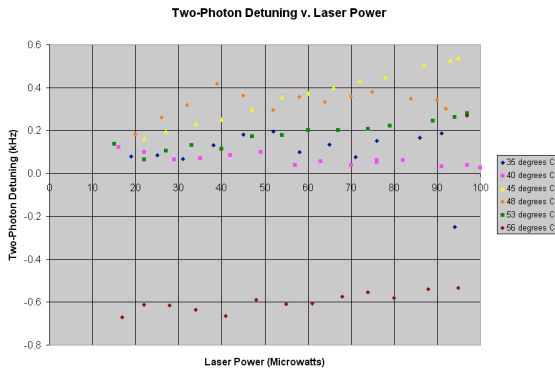

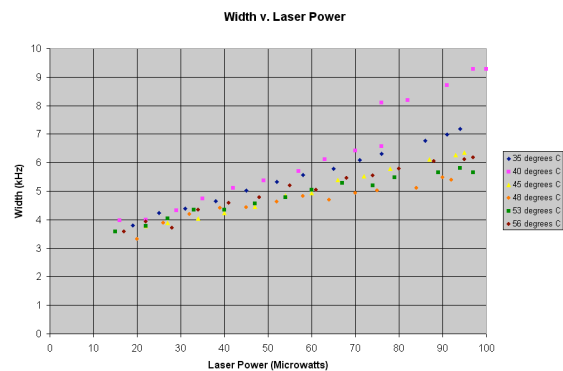
Figure 17: Two-photon detuning versus laser power.

Figure 18: Width versus laser power.

After analyzing the data, we found that 40 degrees Celsius was the correct temperature to use when locking the clock for the second time. Interestingly enough,
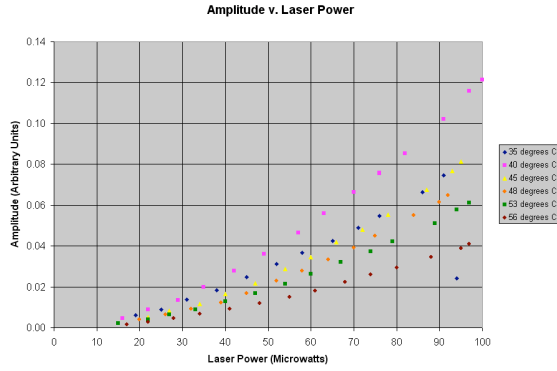
9

Figure 19: Amplitude versus laser power.
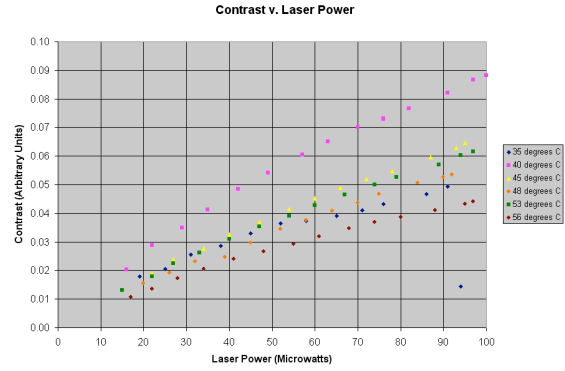

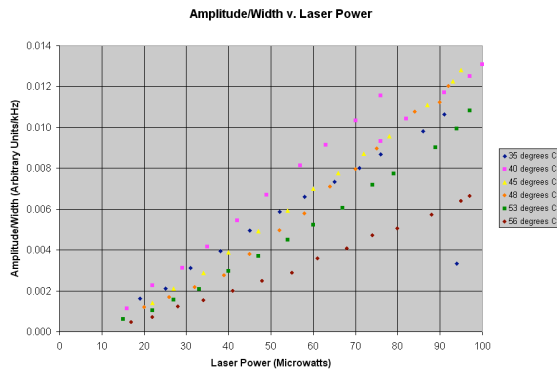Figure 20: Contrast versus laser power.
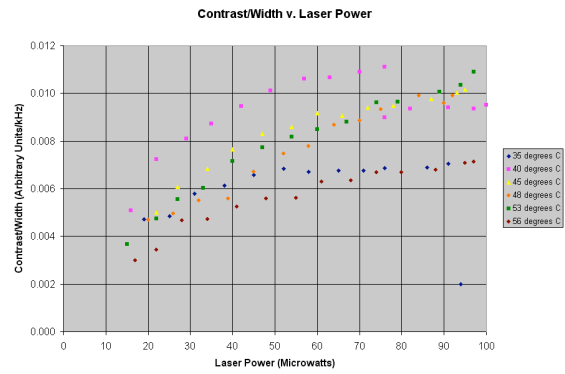

Figure 21: Amplitude/width versus laser power.

Figure 22: Contrast/width versus laser power.

we found the same setting on the potentiometer that controls the temperature of the rubidium cell to be the temperature used in locking the clock. When changing rubidium cells, I reattached the thermistor used to measure the temperature onto the copper cell holder. This gave an offset of a few degrees, but didn't matter in the end.

7   Second Clock Results

Because the work on the second CPT lineshapes data took until the end of the ninth week (out of ten) of the REU program, we have only preliminary data to present for the second clock results. The data does not seem to be much better initially than the first clock results, but there is hope that they can be after understanding and eliminating spurious noise. The best initial Allan variance recorded is 2×10^{-10}, which is slightly better than the first clock results.

8   Conclusion

While the results were not quite what we had hoped for, we have achieved a good understanding of the process to optimize the CPT and clock parameters. We have achieved an Allan variance of 4×10^{-10} with the 15 torr Neon cell, and at least 2×10^{-10} with the 5 torr cell. This leads us to believe that a better Allan variance is possible, just after dealing with noise issues.

9   Acknowledgements

I would like to thank the REU program at William and Mary and Irina Novikova for allowing me to work on this project, and Eugeniy Mikhailov for all of his help with the project. Also to Sergey Zibrov for his ideas on the laser setup, Nate Philips for answering general lab questions, and Chris Carlin for his excellent work on the DAVLL hardware system.

References

[1] N. Belcher and I. Novikova. *Development of a Prototype Atomic Clock Based on Coherent Population Trapping.* The College of William and Mary Senior Thesis. May 2008.

[2] D.K. Serkland, et al. *VCSELs for Atomic Clocks.* Proceedings of the SPIE, Volume 6132, pp. 66-76. 2007.

[3] S. Brandt, et al. *Buffer-gas-induced linewidth reduction of coherent dark resonances to below 50 Hz.* Physical Review A, Third Series, Volume 56, Number 2. August 1997.

[4] S. Knappe, et al. *Characterization of coherent population-trapping resonances as atomic frequency references.* Journal of the Optical Society of America, Volume 18, Number 11, pp. 1545-1553. November 2001.

[5] D. W. Allan, et al. *The Science of Timekeeping.* Hewlett-Packard Application Note 1289. 1997.

[6] D. W. Allan. http://www.allanstime.com/AllanVariance/. February 2004.